ELSEVIER

Contents lists available at ScienceDirect

Quaternary Science Reviews

journal homepage: www.elsevier.com/locate/quascirev



Energy mass balance and flow modeling of early Holocene glaciers in the Queshque valley, Cordillera Blanca, Peru



Nathan D. Stansell ^{a, *}, Bryan G. Mark ^{b, c}, Joseph M. Licciardi ^d, Donald T. Rodbell ^e, Jonathan G. Fairman ^{b, c}, Forrest S. Schoessow ^{b, c}, Tal Y. Shutkin ^{b, c}, Mary Sorensen ^a

- a Department of Geology and Environmental Geosciences, Northern Illinois University, 312 Davis Hall, Normal Road, DeKalb, IL, 60115, USA
- ^b Byrd Polar and Climate Research Center, The Ohio State University, Columbus, OH, 43210, USA
- ^c Department of Geography, The Ohio State University, Columbus, OH, 43210, USA
- ^d Department of Earth Sciences, University of New Hampshire, Durham, NH, 03824, USA
- ^e Geosciences Department, Union College, Schenectady, NY, 12308, USA

ARTICLE INFO

Article history: Received 23 September 2021 Received in revised form 19 January 2022 Accepted 2 February 2022 Available online xxx

Handling Editor: Dr C. O'Cofaigh

ABSTRACT

Our limited knowledge of the timing and pattern of early Holocene climate variability in the tropical Andes hinders our ability to evaluate any potential linkages between low and high latitude oceanicatmospheric dynamics. There is mounting evidence that glaciers in the Peruvian Andes stabilized at times during the early Holocene, suggesting there were periods of colder and/or wetter conditions that interrupted an overall pattern of a warmer and drier climate. Evaluating the global significance of these glacial fluctuations requires that the nature of these apparent cooling events and any shifts in the hydrologic cycle be better quantified. Here we apply a physically-based glacier model to reconstruct and interpret early Holocene-aged paleoglaciers in steady-state with a range of tropical climatic conditions in the Queshque valley of the Cordillera Blanca, Peru (9.8°S). This model uses a LiDAR-based digital elevation model (DEM) and hourly meteorological data as inputs to calculate the fully-distributed surface energy and mass balance (SEMB). This approach allows us to better capture the diurnal range of environmental variability at a spatial resolution that has not been achieved with previous paleo-glacier modeling efforts in this region. A 3-D rendition of paleoglaciers was then developed based on a flow model that responds to the SEMB input, accounting for the valley topography. The model was validated by simulating glaciers that match both field and satellite observations of modern glacier area limits, as well as ice thicknesses that are consistent with recently measured ground-penetrating radar (GPR) profiles of the main glacier tongue. After adjusting for changes in early Holocene global radiation values, and using regional paleoclimate records as constraints for the model, the maximum early Holocene ice limit in the valley dating to ~10.8 (± 0.1) ka was reconstructed using a 3.0 °C cooling and a 25% increase in precipitation relative to today. An up-valley ice extent dating to ~9.4 (±0.3) ka was reconstructed using a 2.8 °C cooling and no change in precipitation amounts relative to today. These results suggest that conditions were cold and wet enough to maintain glaciers at times during the early Holocene, even though a shift to drier conditions combined with modestly warmer temperatures drove a phase of ice retreat from at least ~10.8 to ~9.4 ka. These results suggest that southern tropical temperatures and the hydrologic cycle rapidly reorganized during the early Holocene in conjunction with diminishing ice sheets and shifting environmental conditions in the high latitudes.

© 2022 Elsevier Ltd. All rights reserved.

1. Introduction

The paleo-climatic conditions associated with tropical Andean

* Corresponding author. E-mail address: nstansell@niu.edu (N.D. Stansell). glacier variability during the Holocene remain unclear. This is due, in part, to variable modeling approaches for low latitude glaciers that generally lack detailed climate data (Fernández and Mark, 2016). In contrast to mid-latitude glaciers, the tropical Andes are exposed to strong diurnal temperature and precipitation variability under a strong radiation regime, which is only characterized in subdaily meteorological data (Vincent et al., 2005; Endries et al., 2018).

Likewise, paleo-glacial mass balance models that are commonly forced with linear temperature indices (i.e. positive degree days) might lack the complexity needed to thoroughly evaluate basinspecific tropical Andean glaciers where hydrological conditions play a big role. More complex energy balance models typically account for solar radiation, temperature, humidity, wind speed and precipitation, which is several times the number of variables needed for a temperature index approach (Fernández and Mark. 2016). As such, early research efforts to quantify tropical Andean glacier mass balance models based on fewer variables suggest that paleo-glaciers were more sensitive to temperature variability than precipitation (e.g., Seltzer, 1994). This is in contrast to field-based observations highlighting that modern glaciers in the Cordillera Blanca are indeed highly sensitive to hydrologically controlled variables such as precipitation and relative humidity (Kaser and Georges, 1999; Clark and Barrand, 2020).

Local topography can also lead to a heterogeneity in paleoglacier extents that limits our ability to relate glacier activity to local, regional and global climate patterns (Mark et al., 2005). These hypsometric controls also make it challenging to reconstruct and interpret tropical paleo-glacier snowlines from remnant moraines and other landforms (Benn et al., 2005). A comprehensive modeling approach that integrates climate and topographic factors to simulate paleoglacier mass balance would permit a quantitative assessment of the likely paleoclimate conditions prevailing at times matching the geomorphologic record. A basin-specific technique would also account for regional climate variability as moderated by the local topography (i.e. shading from valley walls, aspect and steepness of the terrain), known to strongly influence mass balance variability for individual mountain glaciers (Mark, 2008). Of course, this approach requires access to quality input data that captures the local environmental conditions affecting the energy balance of tropical glaciers. Fortunately, hourly data from the Cordillera Blanca now exist that can be combined with energy and mass balance models capturing diurnal and longer-term glacier variability (Hock and Holmgren, 2005), and this approach has been adapted and tested for low latitude regions (e.g., Sicart et al., 2011). Likewise, modern observations of glacier-climate-topography contexts constrain modeling approaches to simulate glacier extents in response to specific climate scenarios that can be compared to independently derived proxy evidence (e.g., Kull et al., 2008; Stuart-Smith et al., 2021). By also integrating flow models that generate ice thicknesses from the bed topography along paleoglacier flowlines (e.g., Plummer and Phillips, 2003), these modeling approaches provide methods to test explicitly and quantitatively the nature and extent of climate changes in the confines of local topography that could have caused the glacier mass changes recorded by past glacial deposits.

Here we apply such a modeling approach to reconstruct paleoglaciers in the Queshque valley in the Cordillera Blanca, Peru (Fig. 1) to provide a physical basis for interpreting early Holocene climate conditions. The Queshque valley is an optimal study site given previous research there on glacier chronology (Farber et al., 2005; Rodbell et al., 2008; Stansell et al., 2017) and glacier-climate sensitivity (Mark and Seltzer, 2005). In addition, high resolution digital elevation (Light Detection and Range; LiDAR) and ice thickness ground penetrating radar (GPR) data provide necessary inputs for developing and validating the model (Huh et al., 2017, 2018).

Disentangling the differential drivers of low latitude glacial

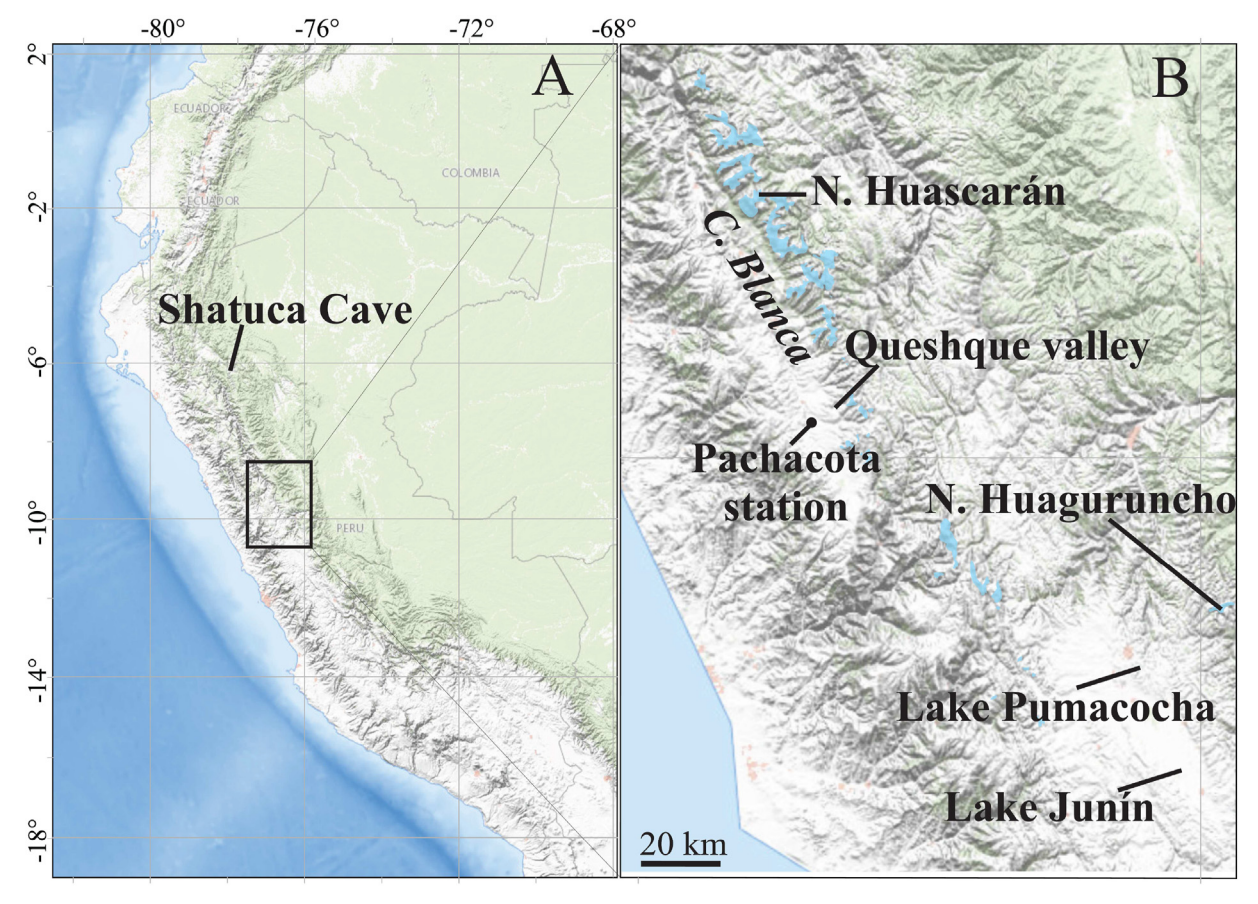


Fig. 1. Location map of Peru (panel A) and inset map of the Cordillera Blanca and other sites mentioned in text (panel B).

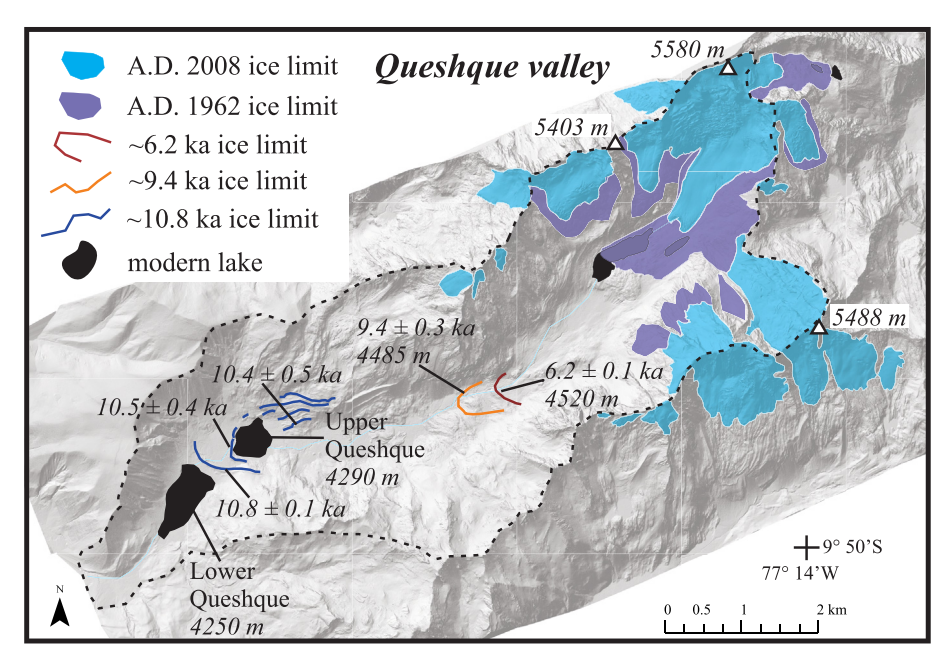


Fig. 2. Map of Queshque valley with averages of ¹⁰Be ages along with historical ice limits (see text). Note that the A.D. 1962 ice limits are only known for within the boundaries of the aerial photograph in Fig. 4. Moraine colors are keyed to plots in Fig. 5 and only the Holocene-aged moraines in the valley are highlighted. Dashed line marks cirque drainage divide

variability on a range of time-scales is important for our general understanding of past climate dynamics. Holocene glacier variability, in particular, has not been thoroughly explored in the context of tropical climate change, making the causes, feedbacks and possible high latitude connections unclear (e.g., Solomina et al., 2015; Novello et al., 2017; Vickers et al., 2020). Despite an overall warmer and drier climate during the early Holocene in the central Andes (Seltzer et al., 2000), there is evidence that glaciers stabilized during brief periods of colder and/or wetter conditions in scattered regions of Peru (e.g., Mark et al., 2017). Specifically, for Queshque, ice cover was much more extensive than today at ~10.8 ka, followed by substantial ice retreat until ~9.4 ka when glaciers stabilized anew (Fig. 2). To date, little attention has focused on the structure of these apparent early Holocene ice advances and/or standstills in the southern tropical Andes (Licciardi et al., 2009). Testing and deploying a physically-based glacier mass model provides a tool for addressing these outstanding questions, while also highlighting knowledge gaps as we evaluate the timing and causes of Holocene tropical climate change.

2. Geographic setting

The Queshque massif is in the southern Cordillera Blanca, Peru (9°48′30″S, 77°15′00″W) (Fig. 1). The Cordillera Blanca has 27 summits over 6000 m in elevation (Ames, 1998), and these glacierized peaks are distributed along the Andean continental divide, forming the headwaters of three principal watersheds that drain either to the Atlantic or Pacific oceans. The range exhibits climatic conditions typical of tropical highlands with both a diurnal temperature range that far exceeds the annual, and a marked seasonality of precipitation (Hastenrath, 1985). By classification, the Cordillera Blanca glaciers are typical of the outer tropics, and experience seasonal accumulation and year-round ablation (Kaser, 2001). During the wet season, the maximum accumulation is coincident with enhanced melt. This regime shifts somewhat during the dry season as lower humidity enhances the relative role of sublimation in addition to melt processes (Wagnon et al., 1999a,

1999b; Winkler et al., 2009). These intense ablation regimes cause glaciers in these regions to exhibit steep vertical mass balance profiles, and mass turnover rates are high (Kaser et al., 1990; Kaser and Georges, 1999).

The orientation of glaciers in the Cordillera Blanca is largely controlled by the structural trend of the Andes, while the distribution of glacier mass also reflects regional gradients in precipitation and solar radiation. Glaciers with a southwest aspect are larger and more numerous than others in the Cordillera Blanca (Ames et al., 1989; Mark and Seltzer, 2005). Generally, glaciers rise from lower to higher elevations in the west as a function of precipitation gradients, but diurnal convection patterns and valley morphology cause a zonal asymmetry in the radiation balance at the ice surfaces (Kaser and Georges, 1997). Individual glaciers with western and southwestern aspects reach lower elevations, locally, in regions where eastern glaciers are more sensitive to this diurnal radiation imbalance. This is the case in the Queshque valley, where glaciers generally extend to lower elevations on southwest-facing slopes, and ice margins east of the divide are restricted to higher levels.

This study focuses on the main Queshque valley that has a generally southwest-facing aspect with an elevation of ~5580 m a.s.l. for the highest peak. The main glacier is fed by multiple cirque basins, and the tongue of this system extends far down-valley relative to the adjacent glaciers. In 2008, ice extended in the valley down to an elevation of ~4750 m a.s.l. (Figs. 2 and 3). The Queshque valley also contains a series of well-preserved moraine sequences and proglacial lakes (Stansell et al., 2013). Lower Queshquecocha (9°49'S, 77°18'W, 4250 m a.s.l.) is dammed by glacial outwash and debris fans. Upper Queshquecocha (9°48′S, 77°18′W, 4290 m asl) is located ~600 m up-valley of the lower lake and is impounded and flanked by distinct lateral-terminal moraines that date to the early Holocene (Stansell et al., 2017). An end moraine just upvalley from Lower Queshquecocha (4285 m a.s.l.) has ¹⁰Be ages that date to 10.8 ± 0.1 ka (n = 3), and further upvalley, a nested pair of end moraines enclosing Upper Queshquecocha dates to 10.5 ± 0.4 ka (n = 4). A group of closely-spaced right-lateral moraines adjacent to Upper Queshquecocha dates to 10.4 ± 0.5 ka

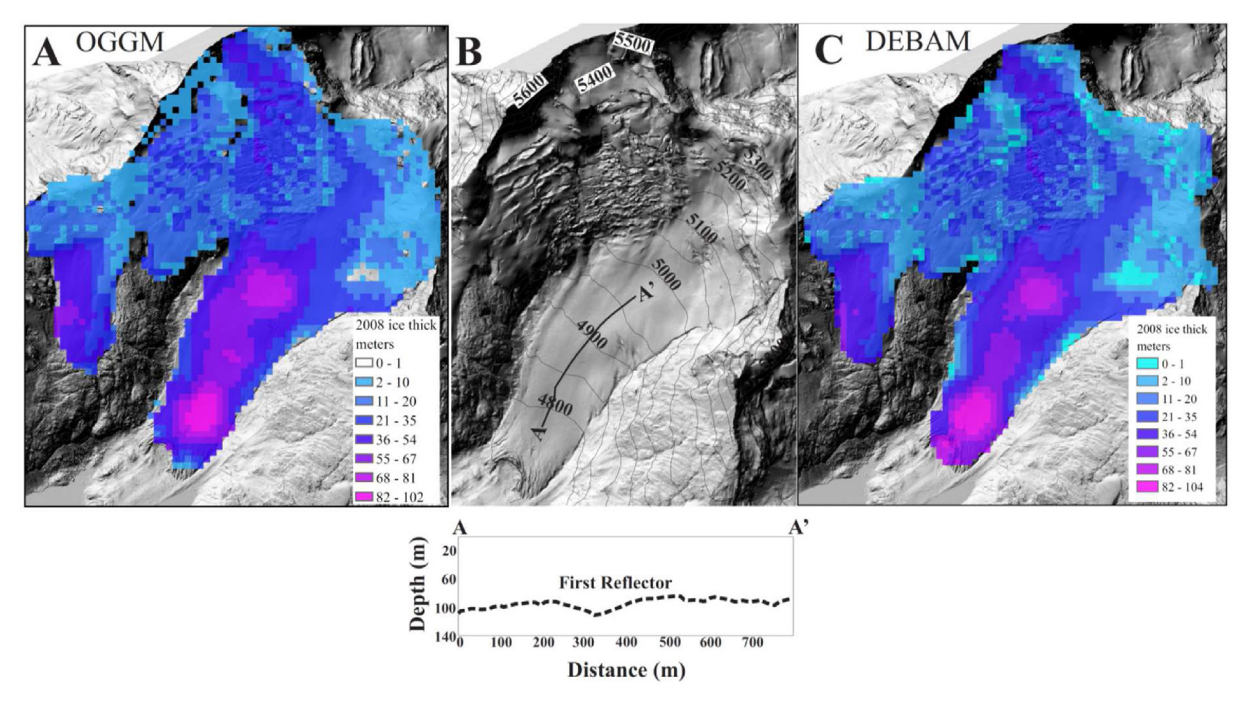


Fig. 3. Panel A - Modeled ice thickness of the present-day glacier using OGGM. Panel B - Contour map of the Main Queshque glacier and ground penetrating radar profile showing ice thickness along the tongue in 2009. The GPR transect line (A-A') is shown for reference. Panel C - Modeled ice thickness when starting with an ice-free DEM.

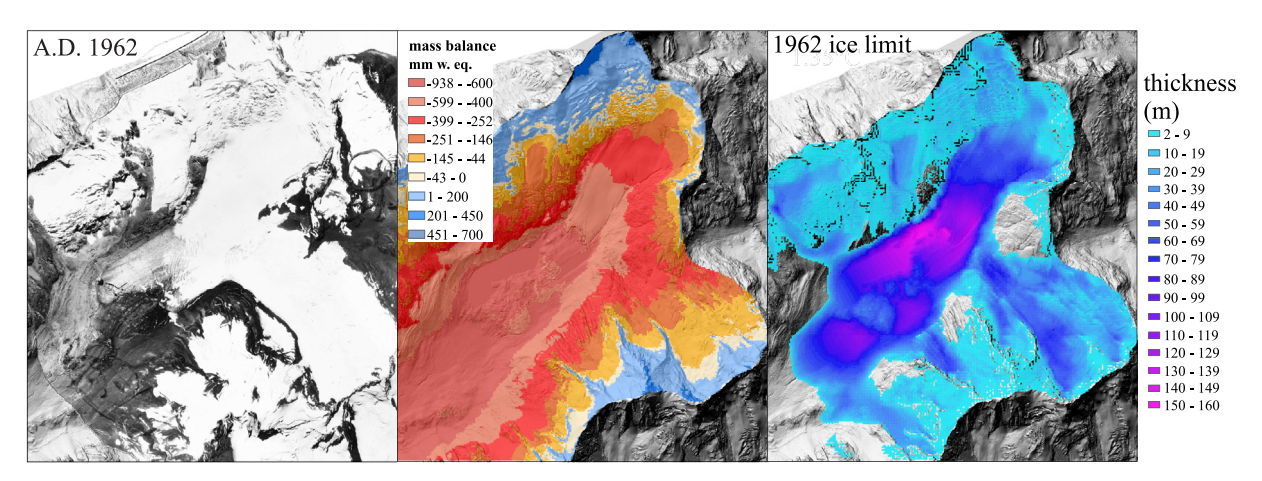


Fig. 4. Aerial photograph (left panel), mass balance model results (middle panel) and modeled ice limits and thicknesses (right panel) for A.D. 1962. This modeled ice limit was driven by a 1.35 °C cooling, no change in precipitation and a wind speed reduction of 2 m/s relative to today.

(n = 6). There are additional early Holocene moraines up-valley from Upper Queshquecocha (~4485 m a.s.l.) that date to ~9.4 \pm 0.3 ka (n = 3) and another group of younger moraine ridges situated between 4680 m and 4520 a.s.l. that date to ~6.2 \pm 0.1 to 0.21 \pm 0.02 ka (n = 7).

3. Data and methods

We combined field observations of modern ice thicknesses with historical climate data and publicly available modeling programs to reconstruct modern and paleo-glaciers. We used a LiDAR-based digital elevation model (DEM) and hourly meteorological inputs from weather station and reanalysis data to develop the baseline surface energy and mass balance (SEMB) model conditions. A 3-D rendition of paleoglaciers was then developed based on a flow model that responds to the SEMB input, accounting for the valley

topography. We compared these modeled changes in ice extent and thickness to observations of late 20th century climate and glacier mass changes. Once validated, we applied this approach to reconstruct early Holocene ice limits using proxy paleoclimate data as constraints.

3.1. Ground penetrating radar (GPR) profile of ice thickness

In June 2009, we gathered GPR data along the Queshque main valley glacier using a 10 Mhz Narod Geophysics type georadar transmitter and oscilloscope receiver (Fig. 3). We collected data at 5 m spacing along transects and georeferenced every 5th or 10th acquisition point (trace) using a hand-held GPS receiver (accurate to ~5–10 m). We calculated a two-way travel time from the first reflection off the bed, and translated this travel time to an ice depth using a constant radar velocity of 0.168 m ns⁻¹. Based on this

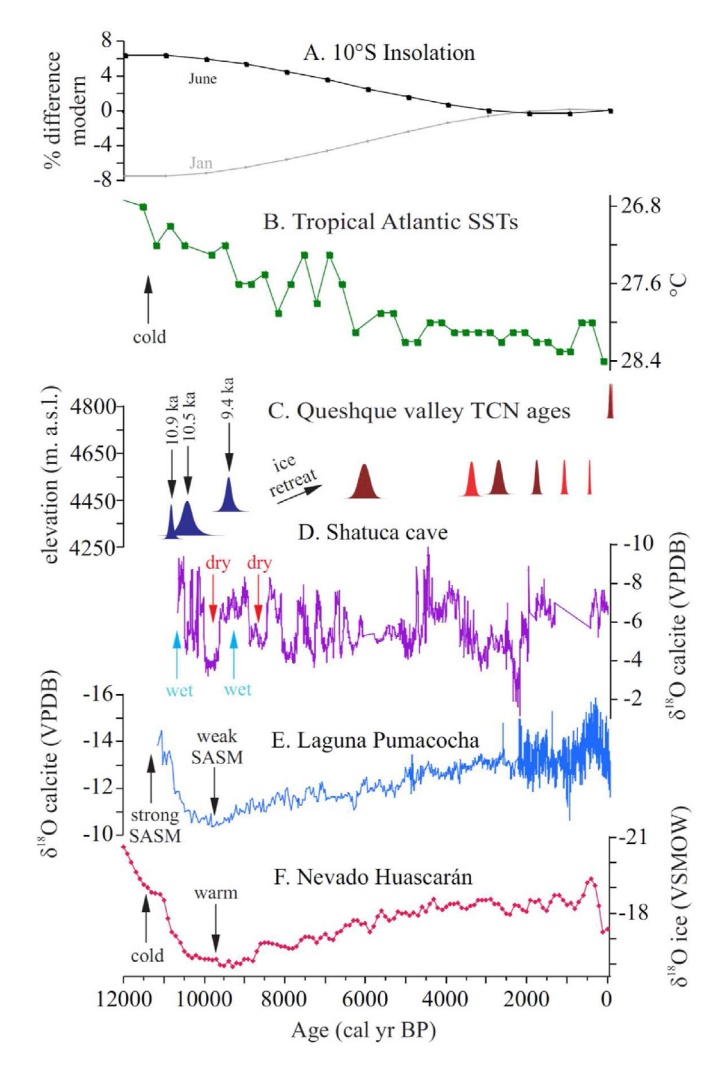


Fig. 5. A: Summer (January) and Winter (June) insolation plotted as percent difference relative to modern (Berger and Loutre, 1991). B: Tropical Atlantic SST reconstructions (Rühlemann et al., 1999). C: TCN age distributions from moraines in Queshque valley, plotted versus elevation (Stansell et al., 2017). D: Stable isotope record from Shatuca Cave with higher and lower values representing dry and wet intervals (Bustamante et al., 2016). E: Stable isotope record from Laguna Pumacocha with lower values representing periods of stronger SASM (Bird et al., 2011). F: Stable isotope record from Nevado Huascarán with lower values representing colder periods (Thompson et al., 1995). These combined datasets suggest that conditions were colder and wetter at times of early Holocene moraine development.

velocity, the one-quarter wavelength resolution of this radar system is 4.2 m. We assumed all reflections came from directly below each trace, and 160 traces were made for a total transect length of ~800 horizontal meters.

3.2. Digital elevation model (DEM) acquisition

In 2008, a (LiDAR) DEM was acquired for the Queshque watershed (Fig. 3). The Airborne LiDAR survey over target glaciers in Cordillera Blanca was conducted within one week during early July 2008 using a Leica ALS60 Airborne Laser Scanner from Leica Geosystems, Switzerland. The Leica ALS60 Airborne Laser Scanner emits and receives 200 kHz max pulse rate of infrared laser light to record ranges from the aircraft platform to the ground. Simultaneously, four GPS base stations (Trimble 5700) were maintained at 20, 40, 80 and 100 km base lengths for post-processed differential correction of LiDAR positions. All corrected data were

georeferenced to the WGS 84 (World Geodetic System, 1984) datum, an Earth fixed global reference frame, including an Earth model and UTM (Universal Transverse Mercator) projection.

3.3. Climate data

Hourly meteorological data, including temperature, precipitation, relative humidity and wind speed were downloaded from Servicio Nacional de Meteorología e Hidrología (Senamhi; https://www.senamhi.gob.pe/servicios/?p=estaciones). The Pachacoto station is at the base of the Queshque watershed (9°51′8.91″S, 77°24′22.03″W; 3733 m a.s.l.), and data are currently available from November 2015 to present. Hourly global radiation, reflected shortwave radiation, net radiation, longwave incoming radiation and longwave outgoing radiation data for Queshque are from ERA5 reanalysis products (www.meteoblue.com/historyplus).

3.4. The mass energy balance model

We applied the fully distributed energy balance model (DEBAM) by Hock and Holmgren (2005), which is available at http://regine.github.io/meltmodel/. As inputs, we used a climate file with hourly data from A.D. 2015 to 2020, as well as gridded surfaces for the watershed, glacier and present-day ice cover that were extracted from the LiDAR data. The model also requires gridded surfaces for aspect and slope values that were calculated using the spatial analyst tools in ArcGIS 10.4.1. The model ran on the Cygwin64 C compiler. The details of the mass balance model are in the supplementary materials.

The climate input file requires some pre-processing of climate data, including the calculation of a precipitation gradient. There is a negative precipitation gradient across many slopes in the Peruvian Andes whereby higher elevation sites on the west-facing, leeward slopes of the Andes experience higher accumulation at elevation (Seltzer, 1992). Based on station data in the Cordillera Blanca (Vuille et al., 2008a), precipitation ranges from ~400 mm/yr at 3000 m a.s.l, and up to ~900 mm/yr at 5000 m a.s.l. The model offers a choice of methods by which to apply a precipitation gradient, either a simple lapse rate or a precipitation change with elevation beyond a certain point. The simple lapse rate method resulted in unrealistic mass balance values and we therefore applied the latter approach. We set the input file with a precipitation value of 960 mm/yr at the base of glacier, and held that value constant across the glacier surface. This near-doubling of precipitation from the elevation of the station to the base of the glacier is similar to what has been used in other alpine modeling approaches (e.g., Maussion et al., 2019).

We use the freezing-level height offset from observed snowline elevation to ascribe a temperature bias input for the model. The freezing-level height is the atmospheric level of the 0 °C isotherm and provides an important constraint on tropical glacier extent; the present-day freezing-level height in the Cordillera Blanca is ~4900 m a.s.l. (Schauwecker et al., 2017), with some individual locations being up to ~5100 m a.s.l. (Rabatel et al., 2013). Here we estimate the freezing level is approximately ~240 m above the snowline, based on Schauwecker et al. (2017). In the Queshque valley, the LiDAR data and Google Earth imagery suggest the snowline is closer to ~5210 m a.s.l. at the start of the ablation season, which equals a freezing height of ~5450 m a.s.l. Linear regression of mean annual air temperatures recorded at regional weather stations identify a lapse rate of 0.65 °C/100 m (Carey et al., 2012; and references therein). The average temperature at the Pachacoto station (3733 m) is 8.7 °C which translates to a freezing height of ~5070 m a.s.l. using the regional lapse rate, a value that it too low compared to observed ice limits. This might be the case because local environmental lapse rates in Andean glacial valleys

are often less steep than regional lapse rates based on linear regression (Ibañez et al., 2021). Regardless, the model allows a temperature bias input and a 2.5 °C warming was applied to create a freezing level that is similar to what is observed specifically at Queshque.

3.5. The flow model

Here we applied the flow model of Plummer and Phillips (2003). The flow model simulates glacial thickness from the input of the mass balance grid. While the mass balance model identifies areas of ablation and accumulation, the flow model predicts the shape, size, and extent that a glacier assumes for those conditions at steady-state. In cases like the Queshque valley with slope values less than 0.2 and multiple cirque basins, a shallow ice approximation approach should produce reliable results (Le Meur et al., 2004). Therefore, the model here applies the standard flow law for ice using the shallow ice approximation while using multiple interpolation methods (see Supplementary Materials).

3.6. Validation

Modern glaciers in the Cordillera Blanca are generally considered to be out of equilibrium with climatic conditions (Hastenrath and Ames, 1995). This recent transience potentially poses a challenge for our attempts to evaluate the efficacy of the model. However, recent ice margin changes in the Cordillera Blanca have been observed in aerial photographs (Mark and Seltzer, 2005; Huh et al., 2017, 2018), and along with modern meteorological data provide a framework for initiating the modeling parameters. Moreover, the relatively rapid mass balance responses to specific El Niño Southern Oscillation (ENSO) events of a few years or less (e.g., Maussion et al., 2015) suggest that the any current disequilibrium of glaciers in Cordillera Blanca might be minimal for this study. For modeling purposes, we therefore assume the Queshque glaciers are at, or near, equilibrium with present-day (A.D. 2008) climate, and no lag time was applied.

In order to validate our coupled modeling approach, we created an ice-free DEM to evaluate how well we could simulate the modern ice conditions with today's climate data using DEBAM. First we used the Open Global Glacier Model (OGGM) ice thickness inversion tool (Farinotti et al., 2009) and the Randolph Glacier Inventory (RGI) 6.0 database (Pfeffer et al., 2017) to develop a 30-m resolution gridded surface of modern ice thickness for the main glacier in the Queshque valley. These thickness estimates (Fig. 3A) were compared to the GPR profile (Fig. 3B). After resampling the LiDAR DEM to 30 m-resolution, the thickness values were then removed from the glacier DEM using the spatial analyst tools in ArcGIS. There has been an average temperature increase in the Cordillera Blanca of ~0.13 °C/decade for the last ~30 years (Schauwecker et al., 2014). We therefore ran DEBAM on the simulated ice-free surface with the A.D. 2018 meteorological data and a cooling of 0.12° to represent the A.D. 2008 conditions. The output of the mass balance model was fed into the flow model (Fig. 3C) for comparison to the GPR transect data (Fig. 3B).

3.7. Sensitivity analysis

The sensitivity of the model to changes in different climate parameters was tested by altering one variable at a time relative to the reference conditions, and observing the resultant changes to the equilibrium-line altitude (ELA), the lowest elevation of glacier extent, maximum and average ice thicknesses, and length of the main glacier (Table 1). Here we define the ELA as the elevation where the calculated mass balance values shift from positive to

negative. For the early Holocene scenarios, we altered temperatures by $\pm\,2\,^{\circ}$ C, precipitation by $\pm50\%$, relative humidity by $\pm20\%$, and the environmental lapse rate values by $\pm0.1\,^{\circ}$ C/100 m of the present day values. The average present day wind speed recorded at the Pachacota station was ~2.6 m/s, and we tested sensitivity by adjusting those values by ±2 m/s. Lastly, we altered cloud cover by $\pm10\%$. We also shifted the elevation to apply the precipitation gradient by ±400 m for the early Holocene scenario. For the modern glacier sensitivity, we followed a similar approach, but with much smaller changes for each environmental variable.

4. Results and discussion

4.1. Measured versus modeled glacier thickness along the Queshque main glacier tongue

The radar profiles indicate that glacier thickness varied from 85 to 115 m along the profile from A to A' in 2009 (Fig. 3B). The maximum glacier thickness was found at a distance of ~330 m upvalley from the terminus along the profile, and the minimum is at ~500 m. The majority of the glacial tongue, however, had consistent observed ice thicknesses that varied between ~95 and 105 m.

A 0.12 °C cooling relative to the modern station data values produced a modeled ice extent that is similar to what is observed in the 2008 LiDAR data, and the modeled ice thickness results are comparable with the field-measured values. The modeled ice thicknesses based on the OGGM ice thickness inversion method were consistently within ~10 m of the measured values (Fig. 3A). The ice thickness results after running DEBAM and the flow model ascribed here (Fig. 3C) resulted in ice thicknesses that were ~10-20 m thinner than the radar profiles (Fig. 3B), which is typical for alpine glacial studies (Linsbauer et al., 2012). For example, modeled ice thicknesses in the Alps have an uncertainty of ~30% compared to GPR measurements (Carturan et al., 2020). While this produces some uncertainties for ice thicknesses, our study is focused more on ice positions and mass balance profiles. We therefore contend that the modeled glacier mass balance and flow models are producing ice margin reconstructions that are consistent with measured field-based observations.

4.2. Historical (A.D. 1962) reconstruction

Aerial photographs and field observations identify changes in the lowest limit of the Queshque glaciers since A.D. 1962. Climate data are also available for this time period, and we used these observations to test the capabilities of the mass balance model to simulate the climate conditions of the historical ice margin positions. For example, aerial photographs from A.D. 1962 indicate that the main Queshque glacier terminated at ~4690 m a.s.l. (Fig. 4). Station data from this region of the Andes suggest that temperatures increased ~0.31 °C/decade from the 1960's to the 1990's, followed by 0.13 °C/decade until 2012 (Schauwecker et al., 2014). There is also evidence of less windy conditions several decades ago in the Cordillera Blanca (Schauwecker et al., 2014). Using this evidence, similar ice limits were produced when using a cooling of 1.35 °C, a 0.65 °C/100 m lapse rate and a 2 m/s reduction in wind speed.

The sensitivity analysis highlights additional model results for the A.D. 1962 glacier from shifting environmental variables (Table 1). Here the ELA, lowest ice limit and ice thickness values only shifted modestly in each model iteration and therefore we focus on changing glacier length for discussion. For example, using a 0.6 °C/100 m lapse rate reduces the glacier length by ~345 m while a value of 0.7 °C/100 m advances the ice margin by ~275 m. Reducing RH by 10% advances the glacier length by ~195 m while

Table 1Mass balance model results and sensitivity analyses for the A.D. 1962 and early Holocene ice extents.

A.D. 1962 – Variable	ELA	Lowest ice limit (m asl)	Max. thick (m)	Avg. thick (m)	Glacier length (m)	Δ Glacier length (m)
baseline conditions -1.4 °C, -2 m/s wind speed	5100	4530	125	18	2750	
+0.2 °C	5120	4540	110	16	2650	-100
−0.2 °C	5100	4520	124	18	2815	65
+10% precip	5100	4520	132	18	2915	165
−10%precip	5120	4550	107	15	2565	-185
+2 m/s wind speed	5120	4540	114	16	2685	-65
−2 m/s wind speed	5100	4520	107	15	2755	5
+10% RH	5140	4655	106	13	2500	-250
−10% RH	5080	4515	136	20	2945	195
Lapse rate: 0.7 °C/100 m	5080	4510	139	20	3025	275
Lapse rate: 0.6 °C/100 m	5140	4660	105	13	2405	-345
Early Holocene – Variable	ELA	Lowest ice limit (m asl)	Max. thick (m)	Avg. thick (m)	Glacier length (m)	Δ Glacier length (m)
−3 °C	4800	4280	285	55	8340	
−5 °C	4720	4270	320	90	10,140	1800
−1 °C	4940	4340	255	35	6910	-1430
. ~	4340	13 10	200			
+50% precip	4740	4270	320	80	9690	1350
				80 30	9690 7160	1350 -1180
+50% precip -50%precip	4740	4270	320			
+50% precip	4740 4920	4270 4300	320 220	30	7160	-1180
+50% precip -50%precip Precip gradient, 2.4x increase @4200 m	4740 4920 4600	4270 4300 4280	320 220 340	30 105	7160 10,670	-1180 2330
+50% precip -50%precip Precip gradient, 2.4x increase @4200 m Precip gradient, 2.4x increase @5000 m	4740 4920 4600 5100	4270 4300 4280 4360	320 220 340 185	30 105 20	7160 10,670 5380	-1180 2330 -2960
+50% precip -50%precip Precip gradient, 2.4x increase @4200 m Precip gradient, 2.4x increase @5000 m Lapse rate: 0.75 °C/100 m Lapse rate: 0.55 °C/100 m	4740 4920 4600 5100 4760	4270 4300 4280 4360 4275 4290 4340	320 220 340 185 300 295 270	30 105 20 65 45 40	7160 10,670 5380 9010 7480 6880	-1180 2330 -2960 670 -860 -1460
+50% precip -50%precip Precip gradient, 2.4x increase @4200 m Precip gradient, 2.4x increase @5000 m Lapse rate: 0.75 °C/100 m	4740 4920 4600 5100 4760 4860	4270 4300 4280 4360 4275 4290	320 220 340 185 300 295	30 105 20 65 45 40	7160 10,670 5380 9010 7480	-1180 2330 -2960 670 -860
+50% precip -50%precip Precip gradient, 2.4x increase @4200 m Precip gradient, 2.4x increase @5000 m Lapse rate: 0.75 °C/100 m Lapse rate: 0.55 °C/100 m +2 m/s wind speed -2 m/s wind speed +20% RH	4740 4920 4600 5100 4760 4860 4880 4740 4860	4270 4300 4280 4360 4275 4290 4340 4280 4300	320 220 340 185 300 295 270 290 275	30 105 20 65 45 40 60 50	7160 10,670 5380 9010 7480 6880 8910 7990	-1180 2330 -2960 670 -860 -1460
+50% precip -50%precip Precip gradient, 2.4x increase @4200 m Precip gradient, 2.4x increase @5000 m Lapse rate: 0.75 °C/100 m Lapse rate: 0.55 °C/100 m +2 m/s wind speed -2 m/s wind speed +20% RH	4740 4920 4600 5100 4760 4860 4880 4740	4270 4300 4280 4360 4275 4290 4340 4280	320 220 340 185 300 295 270 290 275 295	30 105 20 65 45 40	7160 10,670 5380 9010 7480 6880 8910	-1180 2330 -2960 670 -860 -1460 570
+50% precip -50%precip Precip gradient, 2.4x increase @4200 m Precip gradient, 2.4x increase @5000 m Lapse rate: 0.75 °C/100 m Lapse rate: 0.55 °C/100 m +2 m/s wind speed -2 m/s wind speed	4740 4920 4600 5100 4760 4860 4880 4740 4860	4270 4300 4280 4360 4275 4290 4340 4280 4300	320 220 340 185 300 295 270 290 275	30 105 20 65 45 40 60 50	7160 10,670 5380 9010 7480 6880 8910 7990	-1180 2330 -2960 670 -860 -1460 570 -350

increasing RH by the same value shrinks the length by ~250 m. Increasing precipitation by 10% advances the glacier length by ~165 m, but decreasing by the same amount reduces the length by ~185 m. Decreasing temperature by 0.2 °C caused the glacier length to increase by ~65 m while increasing temperature by that amount resulted in only a ~100 m decrease. Finally, decreasing wind speed by 2 m/s advanced the length by ~65 m, but increasing wind speed by the same amount only changed the length by ~5 m.

4.3. Early Holocene reconstructions

There are at least 2 groups of well-defined early Holocene moraines in the Queshque valley. The older sets of Early Holocene moraines are situated at ~4280 m a.s.l. and date to ~10.8 ka (Fig. 2). A younger group of boulders is centered on ~9.4 ka at an elevation of ~4485 m a.s.l. This ~9.4 ka ice limit is just slightly below the Neoglacial extent (~30 m in relief), however, there are prominent weathering posts on the early Holocene moraines that clearly delineate them from any younger ice advances (Rodbell et al., 2012; Stansell et al., 2017).

The sensitivity analysis indicates that multiple paleoclimate scenarios can explain early Holocene glacial variability. Here we focus on length of the main glacier and the ELA and as the most informative values of glacier sensitivity (Table 1). Using a reference glacier that was modeled by only shifting the temperature value by -3 °C, the model yielded a glacier length of ~8340 m and an ELA of ~4800 m a.s.l.. A shallower precipitation gradient reduced the glacier length by ~2960 m and shifted the ELA by ~+300 m, but a steeper gradient increased the length by ~2330 m and shifted the ELA by ~ -200 m. Decreasing temperature by 2 °C caused the glacier length to increase by \sim 1800 m and shifted the ELA by \sim -80 m while increasing temperature by 2 °C resulted in a ~1430 m shorter glacier and shifts the ELA by ~+140 m. Increasing precipitation by 50% adds ~1350 m to the glacier length and shifts the ELA by ~ -60 m, but decreasing by the same amount reduces the length by ~1180 m and shifts the ELA by ~+120 m. Using a 0.55 °C/100 m lapse rate reduces the glacier length by ~860 m and shifts the ELA by ~ -40 m, while a value of 0.75 °C/100 m advances the ice margin by ~670 m and shifts the ELA by ~+60 m. Reducing RH by 20% advances the glacier length by ~450 m and shifts the ELA by ~ -40 m while increasing RH by the same value shrinks the length by ~350 m and shifts the ELA ~+60 m. Increasing wind speed by 2 m/s reduced the length by ~1460 m and shifted the ELA by ~+80 m, but decreasing wind speed by the same amount only changed the length by ~570 m and the ELA by ~ -60 m. Lastly, changes to cloud cover had negligible impacts on the modeled ELA and ice limits.

4.4. Model limitations and assumptions

There are limitations and assumptions in our methods that need to be further discussed when considering this model for paleoclimate reconstructions. Most notably, acquiring reliable meteorological data from the tropical Andes for climate modeling is challenging, and data quality needs to be carefully considered. There is a meteorological station (Pachacota) directly at the foothills of the Queshque valley (Fig. 1) with several continuous years of hourly temperature, precipitation, wind speed and relative humidity data. However, the short duration of available meteorological data allowed us to only simulate several years of mass balance outputs. For example, these data do not capture a full ENSO-cycle, which is a major limitation when trying to capture local climate variability. Likewise, the vertical and east-west gradients in temperature and precipitation need to be better integrated in the model approach, and a more thorough analysis of mass balance variability would likely require decades of climate data from multiple stations in the same valley that are currently unavailable. Nevertheless, we maintain that these data, combined with reanalysis radiation data, provided reasonable results when validating the model.

The limitations of the energy and mass balance model are highlighted in detail in Hock and Holmgren (2005), and here we focus on some of the more notable pitfalls for tropical glaciers. The

model was originally developed for high latitude regions, but has been modified for tropical high mountain glaciers (i.e., the Bolivian Zongo glacier) after adjustments were made to the albedo calculations and pronounced seasonality of radiation dynamics (Sicart et al., 2011). In these regions, the model tends to overestimate snow albedo, which is partially compensated by underestimates of meltwater runoff (Sicart et al., 2011). In addition, the diurnal temperature cycle in the tropics should lead to large subsurface heat fluxes, which the model does not fully resolve. The influences of melt processes and meltwater transfers remain poorly constrained, and the subglacial hydrology in low latitude settings has not been validated (Sicart et al., 2011). Improving most of these parameters requires additional field-based measurements that currently do not exist for the Queshque valley.

A detailed explanation of the issues relating to the development of the flow model techniques is provided in Plummer and Phillips (2003). Most notably, the equations are best suited for plane strain conditions, which has limitations for valley glaciers like the main tongue in the Queshque valley. We are assuming that ice thickness is the primary control by which the glacier interacts with the topography, and that thicknesses calculated using the planestrain flow model are reliable when applying these plane strain equations to a valley glacier. Furthermore, the shape of the glacier at steady-state is primarily a function of the plasticity of the ice and the annual mass balance of the surface. While the shallow ice approximation method might underestimate the influences of longitudinal stresses, this approach works well in valleys like Queshque with multiple cirques and where the slope is < 0.2 (Le Meur et al., 2004). As noted above, it is no surprise that the simulated ice thicknesses are generally less than what is observed in the LiDAR and radar data, which is common for alpine flow models. Nevertheless, the modeled shape and flow patterns match the observed limits and geological evidence.

The biggest limitation of our approach is that the SEMB requires hourly input data for multiple environmental variables that are unknown for paleo-conditions. However, we chose this particular approach because it captures the diurnal cycle and explicitly resolves radiative and turbulent fluxes that are known to be distinct in the tropics. The model is also able to run with the environmental data currently available for our field site. Our goal is not a precise model of ice thickness, rather the position of the terminus at steady state that matches geological evidence. We argue that the model performs well in our validation test and serves as an attempt to quantify the climatic controls of shifting glacial terminus positions. Moreover, the modeled ice flow directions are generally consistent with moraine configurations and inferred paleo-ice positions. We therefore maintain that this is a valid first-order approach to evaluate the sensitivity of paleo-glaciers to a range of climatic variables.

4.5. Model sensitivity to climate variability

The mass balances of glaciers are closely linked to the seasonal cycle of energy balance, and instrument-based measurements confirm that tropical glaciers are highly sensitive to sensible and latent heat fluxes (Wagnon et al., 1999a). Not surprisingly, changes in bulk temperature and shifting lapse rates both had moderately strong impacts on the modeled mass balance (Table 1).

Our model results also highlight the sensitivity to a range of climate variables, in addition to temperature. Varying the precipitation gradient and/or the amount of precipitation had substantial influences on the modeled ice extent. Here again this is consistent with known ice dynamics as the amount and type of precipitation directly influences the proportion of accumulation that is either converted to snow and ice, versus the amount that is ablated. Our

model results are also sensitive to humidity changes, with higher amounts of water vapor promoting a rise in the modeled glacier length and mass loss. This is to be expected as relative humidity tends to impact the latent heat flux at the ice surface, with higher values leading to increased melt rates, and lower values promoting sublimation (Kaser and Georges, 1999; Wagnon et al., 1999a).

The model results presented here indicate that wind speed has a moderately strong secondary influence on mass balance changes. Wind speed is closely associated with latent heat flux, and high rates promote sublimation. We recognize that our wind speed data are from a single automatic weather station at the base of the Queshque valley and these values should be improved with future instrumentation studies. Nevertheless, the model results indicate that higher wind-speeds result in ice margin retreat and a more negative mass balance in the valley. This highlights that sublimation may play an important role in driving ice mass changes.

Sensible heat flux is closely linked to albedo changes that vary greatly throughout the year and interannually in the tropics, as conditions shift during the dry and wet seasons, which are strongly moderately in turn by ENSO. The amount of incoming solar radiation does not vary substantially in tropics annually, and therefore the differences in albedo between slopes are driven largely by changes diurnal variability (Favier et al., 2004). Previous studies regarding the radiation budget for the Queshque glaciers similarly concluded that differences in solar radiation, which is likely related to altered cloud cover, are not a predominant climatic forcing for ice margin changes over the historical period, and that temperature increases provide the required sensible heat transfer needed to drive the observed ice volume changes (Mark and Seltzer, 2005). Notably, adjusting global radiation values to account for orbital forcing during the Early Holocene had only a modest impact on the modeled ice limits, and substantial changes in precipitation and temperature were still required.

4.6. Paleoclimate implications

There was a millennial-scale trend of increasing summer (January) insolation through the Holocene that likely drove an overall pattern of ice retreat, even though there were notable periods of ice advance (Fig. 5). The Lake Junin sediment record suggests that the regional hydroclimate was generally responding to this insolation forcing during the Holocene (Seltzer et al., 2000). Along with these trends, the nearby Huascarán ice core and Pumacocha lake sediment stable isotope records also suggest that conditions were broadly colder and wetter just prior to ~10.8 ka when glaciers terminated down-valley in the Queshque watershed, followed by a pronounced shift to drier and likely warmer conditions when glaciers retreated (Fig. 5). Similar ages of early Holocene glacial variability from nearby Nevado Huaguruncho are also available (Stansell et al., 2015), indicating this was a regional phenomenon and not just a local signal. Notably, the Lake Pumacocha record does not capture substantial centennial scale hydroclimate events during the early Holocene that coincide with the timing of observed glacial variability in the Queshque watershed. This is to be expected, however, because the base of the Pumacocha record contains banded to massive sediments (Bird et al., 2011), which would integrate any possible paleoclimate signal of at least decades to several centuries. On the other hand, the higher resolution Shatuca speleothem record shows a more variable and pronounced pattern of hydroclimate variability during the early Holocene with wetter conditions centered on ~10.6 ka, 10.3 ka and 10.1 ka, around the time glaciers appear to have stabilized in the Queshque valley (Fig. 5). There is also a pronounced aridity event recorded in the Shatuca cave record from ~10.0 to 9.7 ka when there are no apparent cosmogenic ages on moraines at Queshque, suggesting

this was a phase of ice retreat when conditions were drier.

Assuming that conditions were indeed wetter and colder at ~10.8 ka based on the proxy evidence, a modeled ice extent for Queshque was achieved using a 3.0 °C cooling, a 25% increase in precipitation amounts, and adjusting to a less-steep precipitation gradient than today (Fig. 6 and Table 1). We chose this amount because the range of precipitation variability in the monsoon region of Peru during the Holocene was likely between ~15 and 30% (van Breukelen et al., 2008). Regional proxy records suggest that precipitation amounts after ~10.8 ka were then similar to today while temperatures were colder (Fig. 5). Under this scenario, a modeled ice limit was achieved with a cooling of ~2.8 °C and no change in precipitation, which required a slightly steeper precipitation gradient relative to today (Fig. 7 and Table 1). These values should be viewed tentatively, however, as the results of the sensitivity analysis highlight other variables that could offset some of the modeled temperature and precipitation values. It should also be noted that sensitivity here also translates to uncertainty because these climate variables are poorly constrained in both modern and paleo-scenarios. For example, the plausible range in environmental lapse rates remains a topic of debate for both modern (Schauwecker et al., 2014) and paleo-glacier reconstructions (Loomis et al., 2017). It is also unknown how the precipitation gradient, relative humidity and wind speeds might have differed during the early Holocene. Nevertheless, the model produces reasonable results based on our current knowledge of early Holocene climate conditions, and provides a basis for future work and discussion as our knowledge of these environmental variables improves.

Changes in glacier mass balance in the tropical Andes are dynamically linked to regional and synoptic-scale changes in both temperature and hydroclimate (Vuille et al., 2008a). Warming is considered the predominant factor in driving ice mass loss on multi-decadal time-scales in the Cordillera Blanca, at least over the historical period (Mark and Seltzer, 2005). It has also been suggested that there is a strong and significant relationship on interannual time-scales between sea-surface temperature (SST) variations and glacier mass-balance in the Cordillera Blanca (Vuille et al., 2008b). Our results suggest that the temperature difference in the tropical Andes during the early Holocene relative to today (~3 °C) is similar to what has been identified in the available tropical SST reconstructions (~2 °C) (Fig. 5). As the freezing-level height in the tropical atmosphere is strongly correlated with SSTs (Bradley et al., 2009), ocean temperature forcing provides a plausible explanation for atmospheric temperature changes that occurred in the Cordillera Blanca during the early Holocene.

It also appears that there were rapid changes in the SASM during the early Holocene that helped drive glacial variability (Fig. 5), although the mechanism for multi-centennial-scale changes is unclear. Both the northern and southern high latitudes were

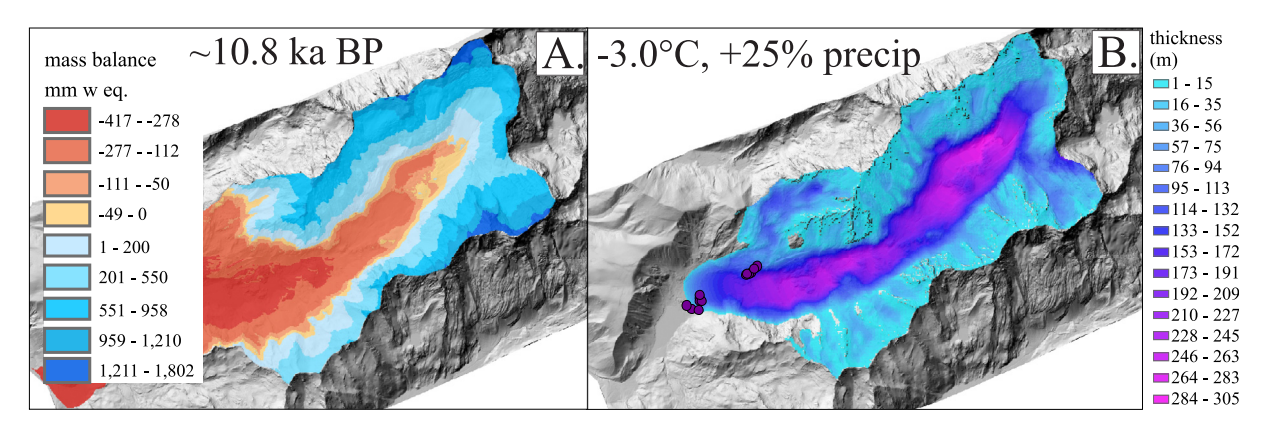


Fig. 6. A - Modeled mass balance \sim 10.8 ka. B - Modeled ice limits and thicknesses for \sim 10.8 ka. The locations of moraine boulders used for dating are shown with purple circles. This ice limit was driven by a 3.0 $^{\circ}$ C cooling and a 25% increase in precipitation.

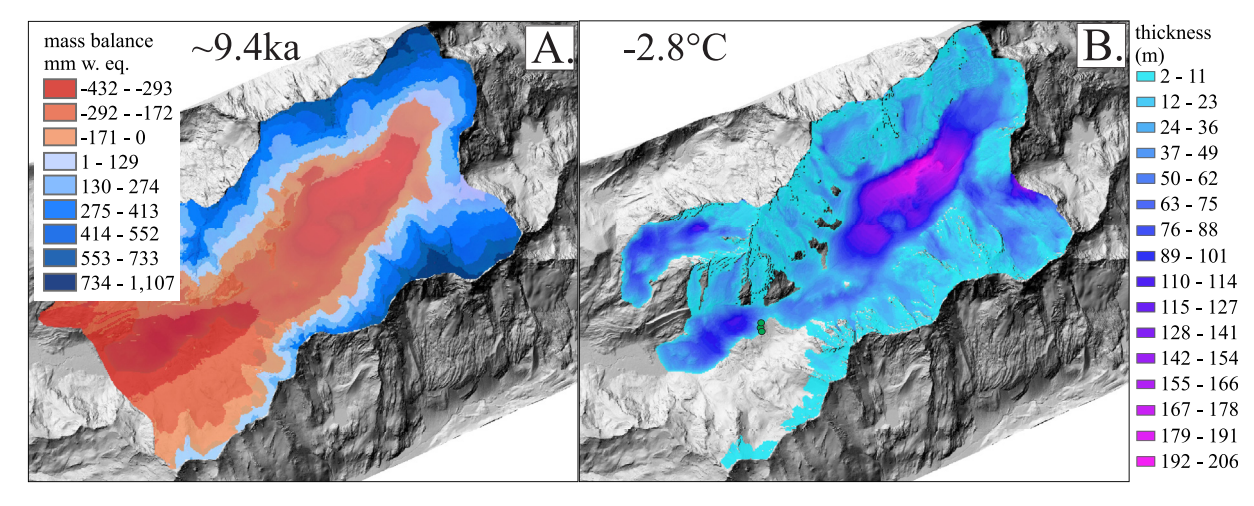


Fig. 7. A — Modeled mass balance for ~9.4 ka. B — Modeled ice limits and thicknesses for ~9.4 ka. The locations of moraine boulders used for dating are shown with green circles (right panel). This modeled ice limit was driven by a 2.8 °C cooling with no change in precipitation relative to today.

experiencing warming during the early Holocene, starting at ~11 ka, possibly associated with changes in thermohaline circulation (Blunier et al., 1997). Cooling in the Northern Hemisphere is generally associated with a latitudinal southerly displacement of the ITCZ, a stronger SASM and wetter conditions in the southern tropical Andes (Vuille et al., 2012). As deglaciation ended, North Atlantic circulation may have then advected heat from the high southern latitudes, leading to overall warming in the Northern Hemisphere (Masson et al., 2000) and possibly drier conditions in the central Peruvian Andes. Brief periods of Early Holocene cooling have been documented in scattered Northern Hemisphere terrestrial records, mostly from Scandinavia (Seppä and Birks, 2001; Heikkilä and Seppä, 2003; Larocque and Hall, 2004), that are coincident with the timing of glacial stillstands in our records. These brief cold periods might provide a mechanism for cooling and increased precipitation in the southern tropical Andes. This is highly speculative, however, as the timing and structure of these Holocene cooling events are poorly resolved (Wanner et al., 2011). Nevertheless, we propose that changes in both southern tropical temperatures and the SASM, possibly connected to shifts in Northern Hemisphere temperature and thermohaline circulation, drove the observed pattern of early Holocene glacial variability in the tropical Peruvian Andes.

5. Conclusions

We have modified and validated a glacier energy mass balance and flow model approach that can be used to evaluate a range of possible climatic conditions associated with past glacial advances for the Queshque valley in the Cordillera Blanca, Peru. The model is sensitive to a range of climatic variables, in addition to topographic influences that control differential amounts of radiation at the ice surface. There are a number of model iterations that are capable of reproducing early Holocene glacial extents in the Queshque region, and better developed independent proxy records from the region will help to refine these methods in order to characterize and isolate the causes of glacial mass balance changes in the Central Andes on a range of time-scales. Nevertheless, these results highlight that glaciers in the Cordillera Blanca are highly sensitive to both temperature and hydrologic controls (precipitation and humidity). Glaciers were likely advanced down valley from their present ice limits at ~10.8 ka under wetter and colder conditions, and then retreated up-valley by ~9.4 ka when the climate was relatively drier and warmer. The results presented here provide further evidence that pronounced changes in the hydrologic cycle, combined with moderate temperature changes, may have driven the early Holocene pattern of glacial variability in the Cordillera Blanca.

Author statement

Nathan D. Stansell: conceptualized modeling, analyzed data, wrote and revised text, Bryan G. Mark: analyzed data, conceptualized modeling, wrote and revised text, Joseph M. Licciardi: analyzed data, conceptualized modeling, wrote and revised text, Donald T. Rodbell: analyzed data, wrote and revised text, Jonathan G. Fairman: analyzed data, conceptualized modeling, wrote and revised text, Forrest S. Schoessow: conceptualized modeling, wrote and revised text, Tal Y. Shutkin: conceptualized modeling, wrote and revised text, Mary Sorensen: conceptualized modeling, wrote and revised text

Declaration of competing interest

The authors declare that they have no known competing

financial interests or personal relationships that could have appeared to influence the work reported in this paper.

Acknowledgements

We thank Adam Clark for assistance with the GPR data. Funding was provided by the U.S. National Science Foundation (EAR-1003711, EAR-1003780, EAR-1344476 and EAR-2002541).

Appendix A. Supplementary data

Supplementary data related to this article can be found at https://doi.org/10.1016/j.quascirev.2022.107414.

References

- Ames, A., 1998. A documentation of glacial tongue variations and lake developments in the Cordillera Blanca. Zeitschrift für Gletscherkumde und Glazialgeologie 34, 1–26.
- Ames, A., Dolores, S., Valverde, A., Evangelista, P., Javier, D., Gavnini, W., Zuniga, J., Gomez, V., 1989. Glacier Inventory of Peru, Part 1: Huaraz, Peru. Jydraandina, SA.
- Benn, D., Owen, L., Osmaston, H., Seltzer, G., Porter, S., Mark, B., 2005. Reconstruction of equilibrium-line altitudes for tropical and sub-tropical glaciers. Ouaternary International 8, 138–139.
- Berger, A., Loutre, M.F., 1991. Insolation values for the climate of the last 10 million years. Quat. Sci. Rev. 10, 297—317.
- Bird, B.W., Abbott, M.B., Rodbell, D.T., Vuille, M., 2011. Holocene tropical South American hydroclimate revealed from a decadally resolved lake sediment δ^{18} O record. Earth Planet Sci. Lett. 310, 192—202.
- Blunier, T., Schwander, J., Stauffer, B., Stocker, T.F., Dallenbach, A., Indermuhle, A., Tschumi, J., 1997. Timing of the antarctic cold reversal and the atmospheric CO2 increase with respect to the younger dryas event. Geophys. Res. Lett. 24, 2683–2686
- Bradley, R.S., Keimig, F., Diaz, H.F., Hardy, D.R., 2009. Recent changes in freezing level heights in the Tropics with implications for the deglacierization of high mountain regions. Geophys. Res. Lett. 36.
- Bustamante, M.G., Cruz, F.W., Vuille, M., Apaéstegui, J., Strikis, N., Panizo, G., Novello, F.V., Deininger, M., Sifeddine, A., Cheng, H., Moquet, J.S., Guyot, J.L., Santos, R.V., Segura, H., Edwards, R.L., 2016. Holocene changes in monsoon precipitation in the Andes of NE Peru based on δ¹⁸O speleothem records. Quat. Sci. Rev. 146, 274–287.
- Carey, M., Huggel, C., Bury, J., Portocarrero, C., Haeberli, W., 2012. An integrated socio-environmental framework for glacier hazard management and climate change adaptation: lessons from Lake 513, Cordillera Blanca, Peru. Climatic Change 112, 733–767.
- Carturan, L., Rastner, P., Paul, F., 2020. On the disequilibrium response and climate change vulnerability of the mass-balance glaciers in the Alps. J. Glaciol. 66, 1034–1050.
- Clark, D., Barrand, N., 2020. Half a Century of Glacier Mass Balance at Cordilleras Blanca and Huaytapallana. Peruyian Andes.
- Endries, J.L., Perry, L.B., Yuter, S.E., Seimon, A., Andrade-Flores, M., Winkelmann, R., Quispe, N., Rado, M., Montoya, N., Velarde, F., 2018. Radar-observed characteristics of precipitation in the tropical high Andes of southern Peru and Bolivia. J. Appl. Meteorol. Climatol. 57, 1441–1458.
- Farber, D.L., Hancock, G.S., Finkel, R.C., Rodbell, D.T., 2005. The age and extent of tropical alpine glaciation in the Cordillera Blanca, Peru. J. Quat. Sci. 20, 759—776.
 Farinotti, D., Huss, M., Bauder, A., Funk, M., Truffer, M., 2009. A method to estimate
- the ice volume and ice-thickness distribution of alpine glaciers. J. Glaciol. 55, 422–430.
- Favier, V., Wagnon, P., Ribstein, 2004. Glaciers of the outer and inner tropics: a different behaviour but a common response to climatic forcing. Geophys. Res. Lett. 31.
- Fernández, A., Mark, B.G., 2016. Modeling modern glacier response to climate changes along the A ndes C ordillera: a multiscale review. J. Adv. Model. Earth Syst. 8, 467–495.
- Hastenrath, S., 1985. Climate and Circulation of the Tropics. C. Reidel Publishing Company, Dordrecht.
- Hastenrath, S.L., Ames, A., 1995. Diagnosing the imbalance of yanamarey glacier In the Cordillera Blanca of Peru. Journal of Geophyscial Research 100, 5105–5112. Heikkilä, M., Seppä, H., 2003. A 11,000 yr palaeotemperature reconstruction from the southern boreal zone in Finland. Quat. Sci. Rev. 22, 541–554.
- Hock, R., Holmgren, B., 2005. A distributed surface energy-balance model for complex topography and its application to Storglaciären, Sweden. J. Glaciol. 51, 25–36.
- Huh, K.I., Baraër, M., Mark, B.G., Ahn, Y., 2018. Evaluating glacier volume changes since the little ice age maximum and consequences for stream flow by integrating models of glacier flow and hydrology in the Cordillera Blanca, Peruvian Andes. Water 10, 1732.
- Huh, K.I., Mark, B.G., Ahn, Y., Hopkinson, C., 2017. Volume change of tropical

- Peruvian glaciers from multi-temporal digital elevation models and volume—surface area scaling. Geogr. Ann. Phys. Geogr. 99, 222—239.
- Ibañez, M., Gironás, J., Oberli, C., Chadwick, C., Garreaud, R.D., 2021. Daily and seasonal variation of the surface temperature lapse rate and 0 C isotherm height in the western subtropical Andes. Int. J. Climatol. 41, E980–E999.
- Kaser, G., 2001. Glacier-climate interaction at low latitudes. J. Glaciol. 47, 195–204.Kaser, G., Ames, A., Zamora, M., 1990. Glacier fluctuations and climate in the Cordillera Blanca, Peru. Ann. Glaciol. 14, 136–140.
- Kaser, G., Georges, C., 1997. Changes of the equilbrium-line altitude in the tropical Cordillera Blanca, Peru, 1930-1950, and their spatial variations. Ann. Glaciol. 24, 344–349.
- Kaser, G., Georges, C., 1999. On the mass balance of low latitude glaciers with particular consideration of the Peruvian Cordillera Blanca. Geogr. Ann. 81A, 643–651
- Kull, C., Imhof, S., Grosjean, M., Zech, R., Veit, H., 2008. Late Pleistocene glaciation in the Central Andes: temperature versus humidity control — a case study from the eastern Bolivian Andes (17°S) and regional synthesis. Global Planet. Change 60. 148—164.
- Larocque, I., Hall, R., 2004. Holocene temperature estimates and chironomid community composition in the Abisko Valley, northern Sweden. Quat. Sci. Rev. 23, 2453–2465.
- Le Meur, E., Gagliardini, O., Zwinger, T., Ruokolainen, J., 2004. Glacier flow modelling: a comparison of the Shallow Ice Approximation and the full-Stokes solution. Compt. Rendus Phys. 5, 709–722.
- Licciardi, J.M., Schaefer, J.M., Taggart, J.R., Lund, D.C., 2009. Holocene glacier fluctuations in the Peruvian Andes indicate northern climate linkages. Science 325, 1677–1679.
- Linsbauer, A., Paul, F., Haeberli, W., 2012. Modeling glacier thickness distribution and bed topography over entire mountain ranges with GlabTop: application of a fast and robust approach. J. Geophys. Res.: Earth Surf. 117.
- Loomis, S.E., Russell, J.M., Verschuren, D., Morrill, C., De Cort, G., Sinninghe Damsté, J.S., Olago, D., Eggermont, H., Street-Perrott, F.A., Kelly, M.A., 2017. The tropical lapse rate steepened during the Last Glacial Maximum. Sci. Adv. 3, e1600815.
- Mark, B., Stansell, N., Zeballos, G., 2017. The Last Deglaciation of Peru and Bolivia, vol. 43, p. 38, 2017.
- Mark, B.G., 2008. Tracing tropical Andean glaciers over space and time: some lessons and transdisciplinary implications. Global Planet. Change 60, 101–114.
- Mark, B.G., Seltzer, G.O., 2005. Evaluation of recent glacier recession in the Cordillera Blanca, Peru (AD 1962-1999): spatial distribution of mass loss and climatic forcing. Quat. Sci. Rev. 24, 2265.
- Masson, V., Vimeux, F., Jouzel, J., Morgan, V., Delmotte, M., Ciais, P., Hammer, C., Johnsen, S., Lipenkov, V.Y., Mosley-Thompson, E., Petit, J.-R., Steig, E.J., Stievenard, M., Vaikmae, R., 2000. Holocene climate variability in Antarctica based on 11 ice-core isotopic records. Quat. Res. 54, 348–358.
- Maussion, F., Butenko, A., Champollion, N., Dusch, M., Eis, J., Fourteau, K., Gregor, P., Jarosch, A.H., Landmann, J., Oesterle, F., Recinos, B., Rothenpieler, T., Vlug, A., Wild, C.T., Marzeion, B., 2019. The open Global Glacier model (OGGM) v1.1. Geosci. Model Dev 12, 909–931.
- Maussion, F., Gurgiser, W., Großhauser, M., Kaser, G., Marzeion, B., 2015. ENSO influence on surface energy and mass balance at Shallap Glacier, Cordillera Blanca, Peru. Cryosphere 9, 1663—1683.
- Novello, V.F., Cruz, F.W., Vuille, M., Stríkis, N.M., Edwards, R.L., Cheng, H., Emerick, S., de Paula, M.S., Li, X., Barreto, E.d.S., Karmann, I., Santos, R.V., 2017. A high-resolution history of the south American monsoon from last glacial maximum to the Holocene. Sci. Rep. 7, 44267.
- Pfeffer, W.T., Arendt, A.A., Bliss, A., Bolch, T., Cogley, J.G., Gardner, A.S., Hagen, J.-O., Hock, R., Kaser, G., Kienholz, C., Miles, E.S., Moholdt, G., Mölg, N., Paul, F., Radić, V., Rastner, P., Raup, B.H., Rich, J., Sharp, M.J., 2017. The Randolph Glacier Inventory: a globally complete inventory of glaciers. J. Glaciol. 60, 537–552.
- Plummer, M.A., Phillips, F.M., 2003. A 2-D numerical model of snow/ice energy balance and ice flow for paleoclimatic interpretation of glacial geomorphic features. Quat. Sci. Rev. 22, 1389.
- Rabatel, A., Francou, B., Soruco, A., Gomez, J., Cáceres, B., Ceballos, J.L., Basantes, R., Vuille, M., Sicart, J.E., Huggel, C., Scheel, M., Lejeune, Y., Arnaud, Y., Collet, M., Condom, T., Consoli, G., Favier, V., Jomelli, V., Galarraga, R., Ginot, P., Maisincho, L., Mendoza, J., Ménégoz, M., Ramirez, E., Ribstein, P., Suarez, W., Villacis, M., Wagnon, P., 2013. Current state of glaciers in the tropical Andes: a multi-century perspective on glacier evolution and climate change. Cryosphere 7, 81–102.
- Rodbell, D.T., Frey, H.M., Manon, M.R., Smith, J.A., McTurk, N.A., 2012. Development of unusual rock weathering features in the Cordillera Blanca, Peru. Quat. Res. 77, 149–158.

- Rodbell, D.T., Seltzer, G.O., Mark, B.G., Smith, J.A., Abbott, M.B., 2008. Clastic sediment flux to tropical Andean lakes: records of glaciation and soil erosion. Quat. Sci. Rev. 27, 1612–1626.
- Rühlemann, C., Mulitza, S., Muller, P.J., Wefer, G., Zahn, R., 1999. Warming of the tropical Atlantic Ocean and slowdown of thermohaline circulation during the last deglaciation. Nature 402, 511.
- Schauwecker, S., Rohrer, M., Acuña, D., Cochachin, A., Dávila, L., Frey, H., Giráldez, C., Gómez, J., Huggel, C., Jacques-Coper, M., 2014. Climate trends and glacier retreat in the Cordillera Blanca. Peru. revisited. Global Planet. Change 119. 85—97.
- Schauwecker, S., Rohrer, M., Huggel, C., Endries, J., Montoya, N., Neukom, R., Perry, B., Salzmann, N., Schwarb, M., Suarez, W., 2017. The freezing level in the tropical Andes, Peru: an indicator for present and future glacier extents. J. Geophys. Res. Atmos. 122, 5172–5189.
- Seltzer, G.O., 1992. Late quaternary glaciation of the Cordillera real, Bolivia. J. Quat. Sci. 7, 87–98.
- Seltzer, G.O., 1994. Climatic interpretation of alpine snowline variations on millennial time scales. Quat. Res. 41, 154–159.Seltzer, G.O., Rodbell, D.T., Burns, S., 2000. Isotopic evidence for late Quaternary
- Seltzer, G.O., Rodbell, D.T., Burns, S., 2000. Isotopic evidence for late Quaternary climatic change in tropical South America. Geology 28, 35–38.
- Seppä, H., Birks, H.J.B., 2001. July mean temperature and annual precipitation trends during the Holocene in the Fennoscandian tree-line area: pollen-based climate reconstructions. Holocene 11, 527–539.
- Sicart, J.E., Hock, R., Ribstein, P., Litt, M., Ramirez, E., 2011. Analysis of seasonal variations in mass balance and meltwater discharge of the tropical Zongo Glacier by application of a distributed energy balance model. J. Geophys. Res. Atmos. 116.
- Solomina, O.N., Bradley, R.S., Hodgson, D.A., Ivy-Ochs, S., Jomelli, V., Mackintosh, A.N., Nesje, A., Owen, L.A., Wanner, H., Wiles, G.C., Young, N.E., 2015. Holocene glacier fluctuations. Quat. Sci. Rev. 111, 9–34.
- Stansell, N.D., Licciardi, J.M., Rodbell, D.T., Mark, B.G., 2017. Tropical oceanatmospheric forcing of late glacial and Holocene glacier fluctuations in the Cordillera Blanca, Peru. Geophys. Res. Lett. 44, 4176–4185.
- Stansell, N.D., Rodbell, D.T., Abbott, M.B., Mark, B.G., 2013. Proglacial lake sediment records of Holocene climate change in the western Cordillera of Peru. Quat. Sci. Rev. 70, 1–14.
- Stansell, N.D., Rodbell, D.T., Licciardi, J.M., Sedlak, C.M., Schweinsberg, A.D., Huss, E.G., Delgado, G.M., Zimmerman, S.H., Finkel, R.C., 2015. Late glacial and Holocene glacier fluctuations at Nevado Huaguruncho in the eastern Cordillera of the Peruvian Andes. Geology 43, 747–750.
- Stuart-Smith, R., Roe, G., Li, S., Allen, M., 2021. Increased outburst flood hazard from Lake Palcacocha due to human-induced glacier retreat. Nat. Geosci. 14, 85–90.
- Thompson, L.G., Mosley-Thompson, E., Davis, M.E., Lin, P.-N., Henderson, K.A., Cole-Dai, J., Bolzan, J.F., Liu, K.-b., 1995. Late glacial stage and Holocene tropical ice core records from Huascarán, Peru. Science 269, 46–50.
- van Breukelen, M.R., Vonhof, H.B., Hellstrom, J.C., Wester, W.C.G., Kroon, D., 2008. Fossil dripwater in stalagmites reveals Holocene temperature and rainfall variation in Amazonia. Earth Planet Sci. Lett. 275, 54.
- Vickers, A.C., Shakun, J.D., Goehring, B.M., Gorin, A., Kelly, M.A., Jackson, M.S., Doughty, A., Russell, J., 2020. Similar Holocene glaciation histories in tropical south America and africa. Geology 49, 140–144.
- Vincent, C., Ribstein, P., Favier, V., Wagnon, P., Francou, B., Le Meur, E., Six, D., 2005. Glacier fluctuations in the Alps and in the tropical Andes. Compt. Rendus Geosci. 337, 97–106.
- Vuille, M., Burns, S.J., Taylor, B.L., Cruz, F.W., Bird, B.W., Abbott, M.B., Kanner, L.C., Cheng, H., Novello, V.F., 2012. A review of the South America monsoon history as recorded in stable isotope proxies over the past two millennia. Clim. Past 8, 1309—1321.
- Vuille, M., Francou, B., Wagnon, P., Juen, I., Kaser, G., Mark, B.G., Bradley, R.S., 2008a. Climate change and tropical Andean glaciers: past, present and future. Earth Sci. Rev. 89, 79–96.
- Vuille, M., Kaser, G., Juen, I., 2008b. Glacier mass balance variability in the Cordillera Blanca, Peru and its relationship with climate and the large-scale circulation. Global Planet. Change 62, 14–28.
- Wagnon, P., Ribstein, P., Francou, B., Pouyaud, B., 1999a. Annual cycle of energy balance of Zongo glacier, Cordillera real, Bolivia. Journal of Geophyscial Research 104, 3907–3923.
- Wagnon, P., Ribstein, P., Kaser, G., Berton, P., 1999b. Energy balance and runoff seasonality of a Bolivian glacier. Global Planet. Change 22, 49–58.
- Wanner, H., Solomina, O., Grosjean, M., Ritz, S.P., Jetel, M.t., 2011. Structure and origin of Holocene cold events. Quat. Sci. Rev. 30, 3109–3123.
- Winkler, M., Juen, I., Mölg, T., Wagnon, P., Gómez, J., Kaser, G., 2009. Measured and modelled sublimation on the tropical Glaciar Artesonraju. Perú. The Cryosphere 3, 21–30.